Inorg. Chem. **2004**, *43*, 5564–5571

Reactivity of Iron(II) 5,10,15,20-Tetraaryl-21-oxaporphyrin with Arylmagnesium Bromide: Formation of Paramagnetic Six-Coordinate Complexes with Two Axial Aryl Groups

Miłosz Pawlicki and Lechosław Latos-Grażyński*

Department of Chemistry, University of Wrocław 14 F. Joliot-Curie Street, Wrocław 50 383, Poland

Received April 6, 2004

Coordination of σ-aryl carbanions by chloroiron(II) 5,20-ditolyl-10,15-diphenyl-21-oxaporphyrin (ODTDPP)$Fe^{II}Cl$ has been followed by ^1H NMR spectroscopy. Addition of pentafluorophenyl Grignard reagent $(C_6F_5)MgBr$ to the toluene solution of (ODTDPP)$Fe^{II}Cl$ in the absence of dioxygen at 205 K resulted in the formation of the high-spin (ODTDPP)-$Fe^{II}(C_6F_5)$. The titration of (ODTDPP)$Fe^{II}Cl$ with a solution of $(C_6H_5)MgBr$ carried at 205 K yields a rare six-coordinate species which binds two σ-aryl ligands $[(ODTDPP)Fe^{II}(C_6H_5)_2]^-$. Warming of the $[(ODTDPP)Fe^{II}(C_6H_5)_2]^-$ solution above 270 K results in the decomposition to mono-σ-phenyliron species (ODTDPP)$Fe^{II}(C_6H_5)$. Controlled oxidation of $[(ODTDPP)Fe^{II}(C_6H_5)_2]^-$ with Br_2 affords (ODTDPP)$Fe^{III}(C_6H_5)Br$, which demonstrates a typical ^1H NMR pattern of low-spin σ-aryl iron(III) porphyrin. The considered oxidation mechanism involves the (ODTDPP)$Fe^{III}(C_6H_5)_2$ species, which is readily reduced to the iron(I) 21-oxaporphyrin, followed by oxidation with Br_2 and replacement of one bromide anion by aryl substituent. The ^1H NMR spectra of paramagnetic iron complexes have been examined in detail. Functional group assignments have been made with the use of selective deuteration. The peculiar ^1H NMR spectral features of $[(ODTDPP)Fe^{II}(p\text{-}CH_3C_6H_4)_2]^-$ (σ-*p*-tolyl: ortho, 30.8; meta, 53.6; para-CH_3, 42.1; furan: –16.0; β-H pyrrole: –27.5, –34.3, –41.8 ppm, at 205 K) are without a parallel to any iron(II) porphyrin or heteroporphyrin and indicate a profound alteration of the electronic structure of iron(II) porphyrin upon the coordination of two σ-aryls.

Introduction

The coordination chemistry of core-modified porphyrins (21-oxaporphyrin, 21-thiaporphyrin, and 21-selenaporphyrin) has been explored for a number of metal ions.[1−19] Relatively little attention has been given to iron heteroporphyrins despite the extensive search for suitable porphyrins and metalloporphyrins to act as biomimetic models of the multiple fundamental biochemical roles played by iron protoporphyrin IX.[20] In the first case studied it was found that high-spin

* Author to whom the correspondence should be addressed. E-mail: LLG@wchuwr.chem.uni.wroc.pl.

(1) Latos-Grażyński, L. Core Modified Heteroanalogues of Porphyrins and Metalloporphyrins. In *The Porphyrin Handbook*; Kadish, K. M., Smith, K. M., Guilard, R., Eds.; Academic Press: New York, 2000; Vol. 2, Chapter 14, pp 361−416.
(2) Broadhurst, M. J.; Grigg, R.; Johnson, A. W. J. *J. Chem. Soc. (C)* **1971**, 3681.
(3) Latos-Grażyński, L.; Lisowski, J.; Olmstead, M. M.; Balch, A. L. *J. Am. Chem. Soc.* **1987**, *109*, 4428.
(4) Latos-Grażyński, L.; Lisowski, J.; Olmstead, M. M.; Balch, A. L. *Inorg. Chem.* **1989**, *28*, 3328.
(5) Lisowski, J.; Grzeszczuk, M.; Latos-Grażyński, L. *Inorg. Chim. Acta* **1989**, *161*, 153.
(6) Latos-Grażyński, L.; Lisowski, J.; Olmstead, M. M.; Balch, A. L. *Inorg. Chem.* **1989**, *28*, 1183.
(7) Lisowski, J.; Latos-Grażyński, L.; Szterenberg, L. *Inorg. Chem.* **1992**, *31*, 1933.
(8) Chmielewski, P. J.; Grzeszczuk, M.; Latos-Grażyński, L.; Lisowski, J. *Inorg. Chem.* **1989**, *28*, 3546.
(9) Chmielewski, P. J.; Latos-Grażyński, L. *Inorg. Chem.* **1992,** *31*, 5231.
(10) Chmielewski, P. J.; Latos-Grażyński, L.; Pacholska, E. *Inorg. Chem.* **1994**, *33*, 1992.
(11) Latos-Grażyński, L.; Lisowski, J.; Chmielewski, P. J.; Grzeszczuk, M.; Olmstead, M. M.; Balch, A. L. *Inorg. Chem.* **1994**, *33*, 192.
(12) Latos-Grażyński, L.; Pacholska, E.; Chmielewski, P. J.; Olmstead, M. M.; Balch, A. L. *Inorg. Chem.* **1996**, *35*, 566.
(13) Chmielewski, P. J.; Latos-Grażyński, L.; Olmstead, M. M.; Balch, A. L. *Chem. Eur. J.* **1997**, *3*, 268.
(14) Chmielewski, P. J.; Latos-Grażyński, L. *Inorg. Chem.* **1998**, *37*, 4179.
(15) Pacholska, E.; Chmielewski, P. J.; Latos-Grażyński, L. *Inorg. Chim. Acta* **1998**, *273*, 184.
(16) Sridevi, B.; Narayanan, S. J.; Srinivasan, A.; Chandrashekar, T. K.; Subramanianan, J. *J. Chem. Soc., Dalton Trans.* **1998**, 1979.
(17) Gebauer, A.; Schmidt, J. A.; Arnold, J. *Inorg. Chem.* **2000**, *39*, 3424.
(18) Hung, C.-H.; Ou, C.-K.; Lee, G.-H.; Peng, S.-M. *Inorg. Chem.* **2001**, *40*, 6845.
(19) Pawlicki, M.; Latos-Grażyński, L. *Inorg. Chem.* **2002**, *41*, 5866.

10.1021/ic0495463 CCC: $27.50
Published on Web 08/12/2004

Chart 1

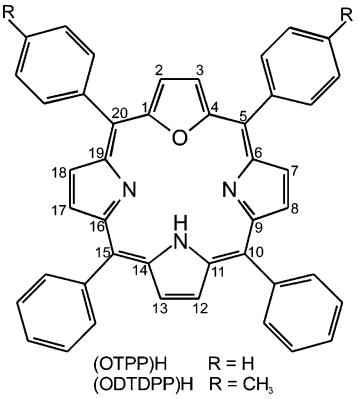

iron(II) 21-thiaporphyrin is a five-coordinate complex where the thiophene ring coordinates in a side-on fashion.[6] Subsequently, the iron complexes of 5,10,15,20-tetraphenyl-21-oxaporphyrin (OTPP)H were investigated (Chart 1).[19]

The charge of the ligand and the size of the coordination cavity of 21-oxaporphyrin resemble those of *N*-alkylporphyrins, for which the coordination of iron was extensively explored.[21] 2-Aza-21-carba-5,10,15,20-tetraarylporphyrin (21-CTPPH$_2$)H, which can be formally treated as a core-modified porphyrin or carbaporphyrin, and its derivatives revealed a remarkable tendency to stabilize peculiar organoiron(II) and organoiron(III) compounds.[22−24]

Considering the dimension of the coordinating core and the feasible in-plane coordination of the furan ring, the 21-oxaporphyrin seems to provide the most suitable environment in the group of heteroporphyrins to explore iron chemistry. In comparison to regular iron porphyrins, the properties of iron 21-oxaporphyrin are expected to reflect the influence of the decreased anionic charge and the replacement of one of the nitrogens by an oxygen atom. In our previous papers, we have studied the coordination of iron by 5,10,15,20-tetraphenyl-21-oxaporphyrin (Chart 1).[19] The skeleton of iron(III) 21-oxaporphyrin (OTPP)Fe^{III}Cl$_2$ is essentially planar. The furan ring coordinates in the η^1 fashion through the oxygen atom, which acquires trigonal geometry, with two axial chloride ligands coordinated apically. One-electron reduction of (OTPP)Fe^{III}Cl$_2$ produced the high-spin five-coordinated (OTPP)Fe^{II}Cl complex **1**. Moreover, titration of (OTPP)Fe^{III}Cl$_2$ or (OTPP)Fe^{II}Cl with *n*-BuLi resulted in the formation of the diamagnetic (OTPP)Fe^{II}(*n*-Bu), which decomposes via a homolytic cleavage of the iron−carbon bond to produce iron(I) 21-oxaporphyrin (OTPP)Fe^{I}.[19]

It is known that iron(III) porphyrins with phenyl groups as axial ligands are paramagnetic intermediates formed during heme degradation by aryl hydrazines.[25] The corresponding model complexes such as (TPP)Fe^{III}Ph (TPP is the dianion of *meso*-tetraphenylporphyrin) can be prepared by the reaction of a Grignard reagent with (TPP)Fe^{III}Cl.[26−29] These compounds can be easily oxidized to form monophenyl iron(IV) porphyrins.[30] Alternatively, the addition of Grignard reagents to iron(III) porphyrin π-cation radicals results in an analogous iron(IV) species.[31] The synthesis and characterization of σ-bonded aryl low-spin iron(III) porphycene were also reported.[32]

The reaction of verdoheme (OEOP)Fe^{III}Br$_2$ (OEOP is the monoanion of octaethyl-5-oxaporphyrin) with Grignard reagents resulted in the replacement of one bromide ligand by an aryl to yield (OEOP)Fe^{III}Br(Ph).[33] An unprecedented six-coordinate verdoheme complex [(OEOP)Fe(Ph)$_2$]$^-$ that coordinates two aryl ligands was detected starting from (OEOP)Fe^{II}Br. Actually, this species was also obtained from (OEOP)Fe^{III}Br$_2$ in the presence of the Grignard reagent in excess, which acts also as the reducing reagent.

^{1}H NMR spectroscopy was shown to be a definitive method for detecting and characterizing iron porphyrins,[34,35] *N*-substituted iron porphyrins,[21,36−39] and hemoproteins on different coordination/oxidation states.[40,41] The essential progress in ^{1}H NMR of paramagnetic hemoproteins can be related to the search for suitable spectroscopic models that mimic the properties encountered in hemoproteins for a given electronic state. Typically the general match between the sign of the chemical shifts in model systems and hemoproteins has been determined for the majority of iron porphyrin ground electronic states. In this paper, we have focused on

(20) Kadish, K. M., Smith, K. M., Guilard, R., Eds. Biochemistry and Binding. In *The Porphyrin Handbook*; Academic Press: New York, 2000; Vol. IV.
(21) Balch, A. L.; Cornman, C. R.; Latos-Grażyński, L.; Olmstead, M. M. *J. Am. Chem. Soc.* **1990**, *112*, 7552.
(22) Chen, W.-C.; Hung, C.-H. *Inorg. Chem.* **2001**, *40*, 5070.
(23) Hung, C.-H.; Chen, W.-C.; Lee, G.-H.; Peng, S.-M. *Chem. Commun.* **2002**, 1516.
(24) Rachlewicz, K.; Wang, S.-L.; Ko, J.-L.; Hung, C.-H.; Latos-Grażyński, L. *J. Am. Chem. Soc.* **2004**, *126*, 4420−4431.
(25) Ortiz de Montellano, P.; Kerr, D. E. *Biochemistry* **1985**, *24*, 1147.
(26) Cocolios, P.; Lagrange, G.; Guilard, R. *J. Organomet. Chem.* **1983**, *253*, 65.
(27) Cocolios, P.; Laviron, E.; Guilard, R. J. *J. Organomet. Chem.* **1982**, *228*, C39.
(28) Ogoshi, H.; Sugimoto, H.; Yoshida, Z.-I.; Kobayashi, H.; Sakai, H.; Maeda, Y. *J. Organomet. Chem.* **1982**, *234*, 185.
(29) Guilard, R.; van Caemelbecke, E.; Tabard, A.; Kadish, K. M. Synthesis, Spectroscopy and Electrochemical Properties of Porphyrins with Metal-Carbon. In *The Porphyrin Handbook*; Kadish, K. M., Smith, K. M., Guilard, R., Eds.; Academic Press: San Diego, CA, 2000; Vol. 3, Chapter 21, pp 295−345.
(30) Balch, A. L.; Renner, M. W. *J. Am. Chem. Soc.* **1986**, *108*, 2603.
(31) Chmielewski, P. J.; Latos-Grażyński, L.; Rachlewicz, K. *Magn. Reson. Chem.* **1993**, *31*, S47.
(32) Kadish, K. M.; Tabard, A.; Van Caemelbecke, E.; Aukauloo, A. M.; Richard, P.; Guilard, R. *Inorg. Chem.* **1998**, *37*, 6168.
(33) Lord, P.; Latos-Grażyński, L.; Balch, A. L. *Inorg. Chem.* **2002**, *41*, 1011−1014.
(34) Walker, F. A. Proton NMR and EPR Spectroscopy of Paramagnetic Metalloporphyrins. In *The Porphyrin Handbook*; Kadish, K. M., Smith, K. M., Guilard, R., Eds.; Academic Press: San Diego, CA, 2000; Vol. 5, Chapter 36, pp 81−183.
(35) Walker, F. A. *Inorg. Chem.* **2003**, *42*, 4526.
(36) Balch, A. L.; Cornman, C. R.; Latos-Grażyński, L.; Renner, M. W. *J. Am. Chem. Soc.* **1992**, *114*, 2230.
(37) Balch, A. L.; La Mar, G. N.; Latos-Grażyński, L.; Renner, M. W. *Inorg. Chem.* **1985**, *24*, 2432.
(38) Balch, A. L.; Chan, Y.-W.; La Mar, G. N.; Latos-Grażyński, L.; Renner, M. W. *Inorg. Chem.* **1985**, *24*, 1437.
(39) Wysłouch, A.; Latos-Grażyński, L.; Grzeszczuk, M.; Drabent, K.; Bartczak, T. *J. Chem. Soc., Chem. Commun.* **1988**, 1377.
(40) La Mar, G. N.; Satterlee, J. D.; De Ropp, J. S. Nuclear Magnetic Resonance of Hemoproteins. In *The Porphyrin Handbook*; Kadish, K. M., Smith, K. M., Guilard, R., Eds.; Academic Press: San Diego, CA, 2000; Vol. 5, Chapter 37, pp 185−298.
(41) Banci, L.; Bertini, I.; Luchinat, C.; Turano, P. Solutions Structures of Hemoproteins. In *The Porphyrin Handbook*; Kadish, K. M., Smith, K. M., Guilard, R., Eds.; Academic Press: San Diego, CA, 2000; Vol. 5, Chapter 39, pp 323−350.

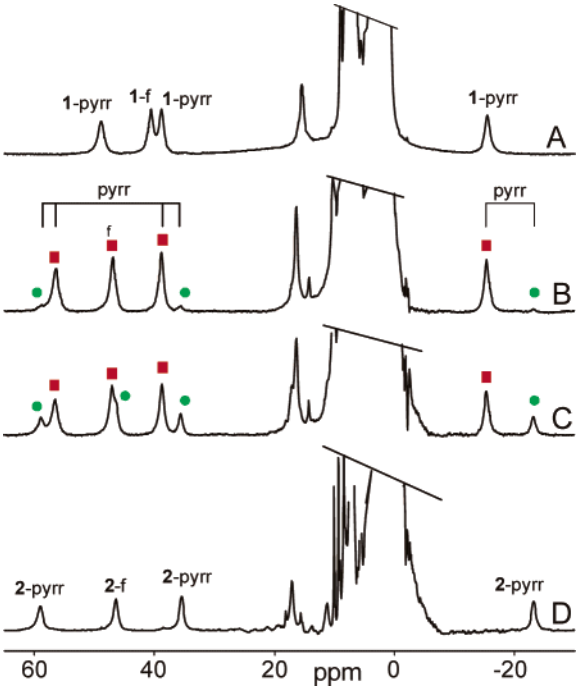

Figure 1. ^{1}H NMR spectra of (ODTDPP)Fe^{II}Cl **1** (toluene-d_8, 205 K) after addition of (C_6F_5)MgBr in diethyl ether: (A) 0 equiv; (B) 0.1 equiv; (C) 0.4 equiv. The resonances of **1**-Et_2O are marked with ■; gradually appearing signals of **2** are marked with ●. Trace D shows the ^{1}H NMR spectrum of **2**. Peak assignments: pyrr, pyrrole resonances; f, furan resonance.

σ-aryl coordination by iron(II) 21-oxaporphyrin using ^{1}H NMR as a spectroscopic probe. In particular, we have detected that the coordination of two axial σ-aryls to the iron(II) 21-oxaporphyrin switches the isotropic shift signs for all β-pyrrole positions, suggesting the presence of the less-common ground electronic state of iron(II).

Results and Discussion

Addition of aryl Grignard reagents (C_6H_5)MgBr, (C_6D_5)MgBr, (C_6F_5)MgBr, (p-$CH_3C_6H_4$)MgBr, and (4-F-C_6H_4)MgBr to the toluene-d_8 solutions (205 K) of (ODTDPP)Fe^{II}Cl **1** resulted in the formation of paramagnetic organoiron species, which have been detected and subsequently characterized by ^{1}H NMR. The ^{1}H NMR resonance assignments have been carried out on the basis of relative intensities and line width analysis. The use of specifically deuterated substrates, (ODTDPP-d_6)Fe^{II}Cl (deuterated at pyrrole positions) and (C_6D_5)MgBr, allowed the assignment of β-H and σ-coordinated phenyl resonances. In each appropriate case the stoichiometry of the σ-phenyl adducts has been unambiguously determined by a careful comparison of resonance intensities assigned to the equatorial macrocycle and σ-aryl protons, respectively.

Figure 1 shows the ^{1}H NMR spectrum that was obtained at 205 K during the titration of a solution of (ODTDPP)Fe^{II}Cl **1** in toluene-d_8 with a solution of (C_6F_5)MgBr in diethyl ether. The titration reflects the combination of two factors: the iron/pentafluorophenyl ratio and the solvent composition. Understanding of this process is of particular importance since the σ-aryliron complex is typically prepared in the presence of diethyl ether (the solvent for Grignard reagents). The effect of the ether can be seen by comparing trace A of Figure 1 with trace B, which shows the sample to which the first portion of the titrant has been added. The presence of ether results in the shift of all resonances (Figure 1, trace B), and their positions remain constant in the further titration steps. Actually, in the independent experiment it has been demonstrated that the addition of diethyl ether alone causes identical spectroscopic changes. The detected transformation is ascribed to the formation of high-spin (ODTDPP)Fe^{II}Cl(Et_2O) **1**-Et_2O, favored by the low-temperature conditions of the experiment. Ethers do not act as strong ligands toward iron porphyrins. Nevertheless the coordination of tetrahydrofuran to acetylide iron(III) porphyrins was previously reported.[42] Gradual addition of the Grignard reagent also produces a set of new resonances, already seen in trace B as the minor component, which differs from **1** or **1**-Et_2O only by the shift values, affording a straightforward assignment of 21-oxaporphyrin resonances of (ODTDPP)Fe^{II}(C_6F_5) **2**. Once formed, the species is stable in the whole investigated temperature range (203−270 K). Thus the spectroscopic evidence is clearly consistent with the replacement of the chloride ligand by the apically σ-coordinating C_6F_5 group. Presumably the molecule of ether is coordinated in the trans position to the carbanion. It has been shown previously that the $C_6F_5^-$ anion tends to stabilize the high-spin σ-aryliron(III) porphyrins contrary to $C_6H_5^-$, where the low-spin ground electronic state of iron(III) is preferred.[32,43,44] Here, these preferences are extended to the iron(II) oxidation level as seen for the (ODTDPP)Fe^{II}(C_6F_5)−(ODTDPP)Fe^{II}-(C_6H_5) pair (see below).

The titration of (ODTDPP)Fe^{II}Cl **1** with a solution of (p-$CH_3C_6H_4$)MgBr in diethyl ether instead of (C_6F_5)MgBr yields a completely different picture as illustrated in Figure 2. Initially **1**-Et_2O has been detected. Upon subsequent addition of the titrant, the spectrum of **1**-Et_2O gradually disappears, and the spectrum of a new species, designated as [(ODTDPP)Fe^{II}(p-$CH_3C_6H_4$)$_2$]$^-$ **3**-Me is observed as seen in trace A of Figure 2. The new species is stable to the addition of further quantities of arylmagnesium bromide. The resonances of **3**-Me have been assigned on the basis of their relative integrated intensities and comparison with ^{1}H NMR spectra of the specifically deuterated sample [(ODTDPP-d_6)Fe^{II}(p-$CH_3C_6H_4$)$_2$]$^-$ **3**-Me-d_6 and [(ODTDPP)Fe^{II}(p-$CH_3C_6H_4$)$_2$]$^-$ **3**-Me. The species **3** presents the ^{1}H NMR pattern without a parallel to any iron porphyrin or heteroporphyrin, as clearly seen by comparison of the data gathered in Table 1. The bis(σ-aryl) adduct **3** shows strongly upfield shifted pyrrole and furan resonances. The acquisition of a COSY spectrum for [(ODTDPP)Fe^{II}(p-$CH_3C_6H_5$)$_2$]$^-$ **3**-Me has allowed the pyrrole resonances to be paired. A cross-peak is observed between the pyrrole resonances at −27.6 and −34.4 ppm

(42) Balch, A. L.; Latos-Grażyński, L.; Noll, B. C.; Phillips, S. L. *Inorg. Chem.* **1993**, *32*, 1124.
(43) Tabard, A.; Cocolios, P.; Lagrange, G.; Gerardin, R.; Hubsch, J.; Lecomte, C.; Zarembowitch, J.; Guilard, R. *Inorg. Chem.* **1988**, *27*, 110.
(44) Kadish, K. M.; Van Caemelbecke, E.; Gueletii, E.; Fukuzumi, S.; Miyamoto, K.; Suenobu, T.; Tabard, A.; Guilard, R. *Inorg. Chem.* **1998**, *37*, 1759.

Table 1. Chemical Shifts of Organoiron Porphyrin Complexes[a]

compound	furan	pyrrole	σ-aryls *o*	σ-aryls *m*	σ-aryls *p*	ref
(ODTDPP)Fe^{II}Cl **1**	40.5	48.9, 38.8, −15.6				
(ODTDPP)Fe^{II}Cl(Et$_2$O) **1**-Et$_2$O	46.9	56.4, 38.7, −15.5				
(ODTDPP)Fe^{II}(C$_6$F$_5$) **2**	46.4	58.9, 35.5, −23.1				
[(ODTDPP)Fe^{II}(C$_6$H$_5$)$_2$]$^-$ **3**-H[b]	−15.3	−26.5, −32.7, −39.9	32.3	52.2	−1.8	
[(ODTDPP)Fe^{II}(4-F−C$_6$H$_5$)$_2$]$^-$ **3**-F	−17.2	−33.2,−34.0,−42.9	14.1	46.7	-	
[(ODTDPP)Fe^{II}(*p*-MeC$_6$H$_5$)$_2$]$^-$ **3**-Me	−16.0	−27.5, −34.3, −41.8	30.8	53.6	42.1	
[(ODTDPP)Fe^{II}(C$_6$H$_5$)(*p*-MeC$_6$H$_5$)$_2$]$^-$ **3**-(H,Me)[b]	−14.8	−26, −32.2, −39.2	33.7	51.9	42.2	
			27.2	51.2		
(ODTDPP)Fe^{II}(C$_6$H$_5$) **4**	9.09, 8.94, 8.79, 8.76		no[l]	5.84	6.02	
(ODTDPP)Fe^{III}(C$_6$H$_5$)Br **5**[c]	−10.0	−22.9, −28.0, −42.3	−100.2	14.5	−37.8	
(STPP)Ni^{II}(C$_6$H$_5$)[d]	−58.0[f]	87.0, 35.4, 2.0	616[e]	170[e]	76[e]	9
[(O$_2$TPP)Ni^{II}(C$_6$H$_5$)$_2$][b]	−31.35	−143.05	5.5[e]	−4.47		14
[(OEOP)Fe(C$_6$H$_5$)$_2$]$^-$ [d,g]			−6.5	43	10	33
(TTP)Fe^{III}(C$_6$H$_5$)[h,i]		−28	−111	20	−30	46
(TPP)Fe^{III}(*p*-Tol)[h,b]		−30	−113	23	89	46
(TTP)Fe^{IV}(C$_6$H$_5$)Br[h,i]		−60		−71	−113	30
(TPP)Fe^{IV}(*p*-Tol)Br[h,b]		−63	−290	−67	114	30
(TPP)Ru^{III}(C$_6$H$_5$)[j,k]		−30.94	−89.53	51.65	−57.47	47
(TPP)Ru^{IV}(C$_6$H$_5$)$_2$[h,j]		8.35	1.31	5.22	5.63	47

[a] All values were obtained at 205 K (toluene-d_8) unless otherwise indicated, [b] 215 K, [c] 243 K, [d] 203 K, [e] ^{2}H NMR, [f] Thiophene, [g] CD_2Cl_2, [h] $CDCl_3$, [i] 223 K, [j] RT, [k] Benzene. [l] no, not observed. This signal is expected in the region of intense, solvent signals (1−2 ppm).

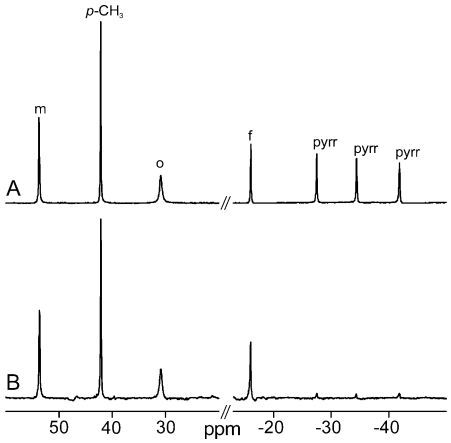

Figure 2. ^{1}H NMR spectra of (A) [(ODTDPP)Fe^{II}(*p*-CH$_3$C$_6$H$_4$)$_2$]$^-$ **3**-Me (^{1}H NMR, toluene-d_8, 205 K); (B) [(ODTDPP-d_6)Fe^{II}(*p*-CH$_3$C$_6$H$_4$)$_2$]$^-$ **3**-d_6 (^{1}H NMR, toluene, 205 K). Peak labels: pyrr, pyrrole resonances; f, furan resonance; o, m, *p*-CH$_3$, resonances of ortho, meta, and para signals of σ-*p*-tolyl rings.

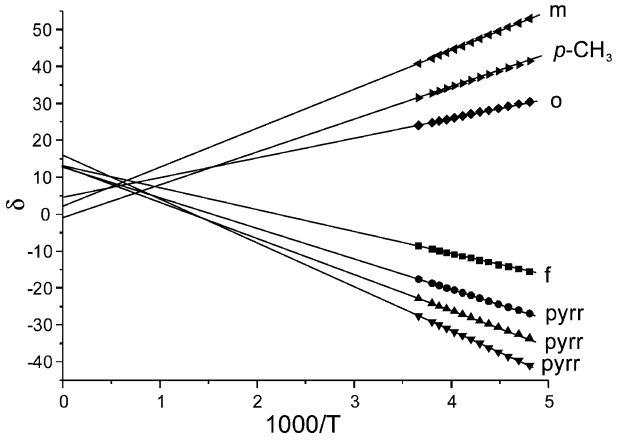

Figure 3. Curie plots (chemical shifts vs 1/*T*) for pyrrole, furan, and σ-(*p*-tolyl) of [(ODTDPP)Fe^{II}(*p*-CH$_3$C$_6$H$_5$)$_2$]$^-$ **3**-Me in toluene-d_8.

(205 K), which have been assigned to the unequivalent, vicinal coupled H(7)−H(8) (H(17)−H(18)) pairs of protons. The most upfield pyrrole resonance at −41.8 (205 K) has been assigned to H(12), H(13) by default. The ortho and meta proton resonances of σ-tolyl are located in the low-field part of the spectrum at 30.9 and 53.7 ppm (205 K). The assumption of metal-centered paramagnetic relaxation yields to the anticipation that the line width for the various protons will be proportional to r^{-6} where the *r* is the distance from the iron to the proton in question.[45] Thus these two resonances could be differentiated by the line widths, which are expected to be larger for the ortho resonance due its proximity to the iron. The resonance observed at 42.2 ppm (205 K) was assigned to the *p*-CH$_3$ group by comparison of the relative intensities of the axial ligand resonances. The downfield position of *p*-CH$_3$ complies with the unusual spectroscopic pattern of the σ-coordinated aryl ligand in **3**-Me. The other Grignard reagents applied in titration lead to the analogus bis-aryl complexes [(ODTDPP)Fe^{II}(C$_6$H$_5$)$_2$]$^-$ **3**-H and [(ODTDPP)Fe^{II}(4-F−C$_6$H$_4$)$_2$]$^-$ **3**-F as confirmed by the similarity of their ^{1}H NMR spectra (Table 1).

A plot of the chemical shifts of the ^{1}H NMR resonances of [(ODTDPP)Fe^{II}(*p*-Tol)$_2$]$^-$ **3**-Me versus 1/*T* are linear within the accessible temperature range (from 203 to 273 K) over which **3**-Me could be observed (Figure 3).

The pattern of resonances seen in Figure 2 is consistent with the formation of [(ODTDPP)Fe^{II}(*p*-CH$_3$C$_6$H$_4$)$_2$]$^-$ **3**-Me as shown in Scheme 1. Consideration of the integrated intensities of the σ-aryl resonances and the integrated intensities of the pyrrole and furan resonances indicates that there are two aryl groups axially bound to the iron(II) 21-oxaporphyrin. To confirm this point, the experiments with (C$_6$H$_5$)MgBr, (*p*-CH$_3$C$_6$H$_4$)MgBr, and a mixture of (C$_6$H$_5$)-MgBr and (*p*-CH$_3$C$_6$H$_4$)MgBr (1:1 molar ratio) were performed. All spectra were collected at the same temperature with similar concentrations of reagents. The results are shown

(45) Swift, T. J. The Paramagnetic Linewidth. In *NMR of* Para*magnetic Molecules. Principles and Applications*; La Mar, G. N., Horrocks, W. D., Jr., Holm, R. H., Eds.; Academic Press: New York, 1973; Chapter 2, pp 53−83.

Scheme 1. Coordination of σ-Aryl Ligand by Iron(II) 21-Oxaporphyrin

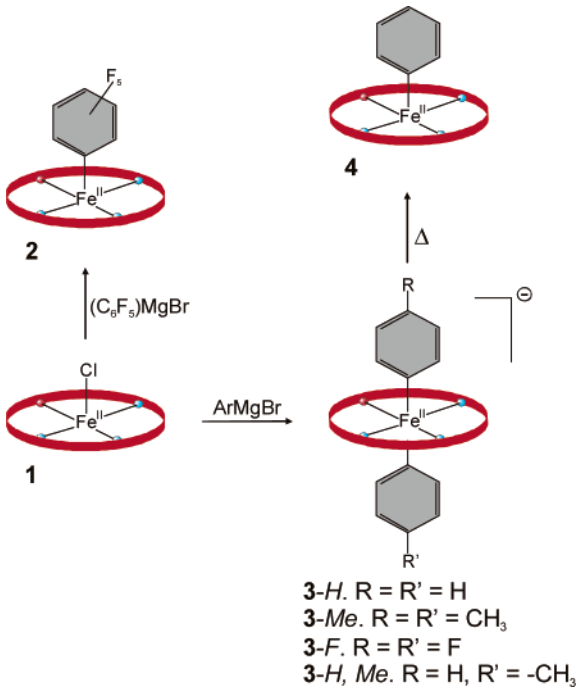

in Figure 4. Trace A shows the spectrum of $[(ODTDPP)Fe^{II}(C_6H_5)_2]^-$ **3**-H while trace C shows the corresponding portion of the spectrum of $[(ODTDPP)Fe^{II}(p\text{-}CH_3C_6H_4)_2]^-$ **3**-Me. Trace B shows the spectrum obtained by adding a 1:1 mixture of $(C_6H_5)MgBr$ and $(p\text{-}CH_3C_6H_4)MgBr$ to $(ODTDPP)Fe^{II}Cl$. In addition to the resonances of **3**-H and **3**-Me, there are new resonances assigned to the mixed-ligand species, $[(ODTDPP)Fe^{II}(C_6H_5)(p\text{-}CH_3C_6H_4)_2]^-$ **3**-(H,Me). The signals of **3**-(H,Me) include a methyl resonance at 42.2 ppm (215 K) for the *p*-tolyl group, two meta resonances (51.9 and 51.2 ppm, 215 K), and two ortho resonances (33.7 and 27.2 ppm, 215 K). The mixed species **3**-(H,Me) contains two different σ-aryl ligands. Consequently, a single meta (ortho) resonances of **3**-Me (**3**-H) is replaced for **3**-(H,Me) by two meta (ortho) resonances of the same intensity coming from the σ-phenyl and σ-(*p*-tolyl) of **3**-(H,Me), respectively. A complete set of pyrrole and furan resonances has been also assigned to **3**-(H,Me) at the upfield region of the spectrum (Figure 4, trace B).

Warming of a solution of $[(ODTDPP)Fe^{II}(C_6H_5)_2]^-$ **3**-H above 270 K results in the disappearance of the resonances of this complex in a matter of minutes. The decomposition product has been identified as the diamagnetic $(ODTDPP)Fe^{II}(C_6H_5)$ **4**. Three resonances are expected for a σ-coordinated phenyl, but only two of them are observed. That resonances are upfield shifted by the macrocyclic ring currents (Table 1), similarly as in metalloporphyrins bearing an axial aryl ligand.[47] The pyrrole and furan resonances are located at 8.79, 8.76 (H2(H3), H12(H13)) 9.09, 8.94 (H7(H18), H8(H17)) ppm. Integration of the β-H and the axial ligand resonances indicates that one axial ligand is

(46) Balch, A. L.; Renner, M. W. *Inorg. Chem.* **1986**, *25*, 303.
(47) Ke, M.; Sishta, C.; James, B. R.; Dolphin, D.; Sparapany, J. W.; Ibers, J. A. *Inorg. Chem.* **1991**, *20*, 4766.

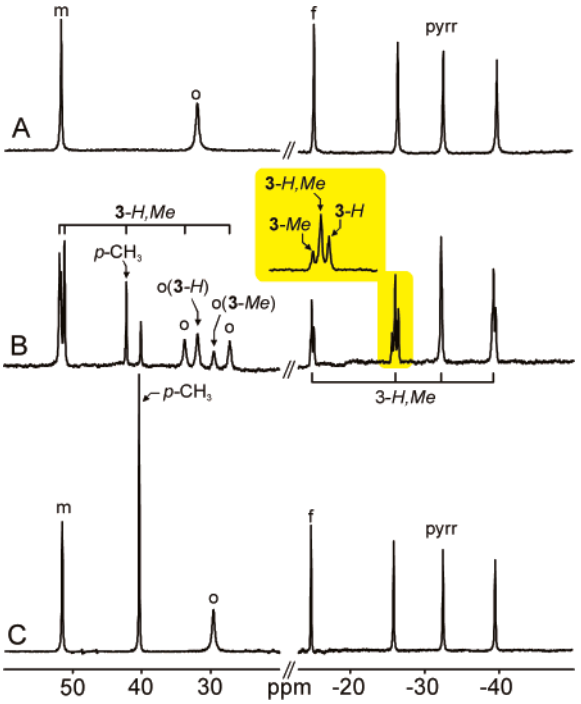

Figure 4. ^1H NMR spectra of (A) $[(ODTDPP)Fe^{II}(C_6H_5)_2]^-$ **3**-H; (C) $[(ODTDPP)Fe^{II}(p\text{-}CH_3C_6H_4)_2]^-$ **3**-Me; and (B) a mixture of $[(ODTDPP)Fe^{II}(C_6H_5)_2]^-$ **3**-H, $[(ODTDPP)Fe^{II}(p\text{-}CH_3C_6H_4)_2]^-$ **3**-Me, and $[(ODTDPP)Fe^{II}(C_6H_5)(p\text{-}CH_3C_6H_4)_2]^-$ **3**-(H,Me) at 215 K. In trace B, the resonances of the mixed-ligand complex, $[(ODTDPP)Fe^{II}(C_6H_5)(p\text{-}CH_3C_6H_4)_2]^-$ **3**-(H,Me)- are marked. Inset in trace B presents the selected region where the presence of three lines assigned to three different species is clearly observed.

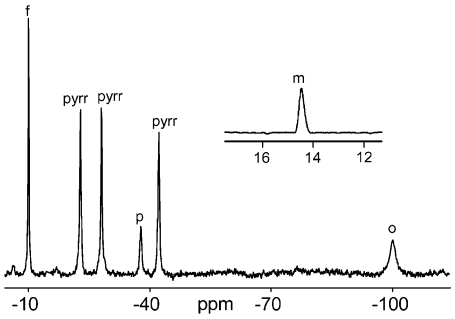

Figure 5. Upfield region of ^1H NMR spectrum of $[(ODTDPP)Fe^{III}(C_6H_5)\text{-}Br]$ **5** (toluene-d_8, 243 K) obtained after addition of Br_2 to $[(ODTDPP)Fe^{II}(C_6H_5)_2]^-$ **3**-H. Inset presents the downfield region of spectra with meta signal of the axial phenyl. Peak labels: pyrr, pyrrole resonances; f, furan resonance; o, m, p, resonances of ortho, meta, and para signals of σ-phenyl ring.

present in the iron(II) complex (Table 1). The coordination of σ-aryl ligand by iron(II) 21-oxaporphyrin examined in this study are summarized in Scheme 1.

The newly detected $[(ODTDPP)Fe^{II}(C_6H_5)_2]$- **3**-H is unstable in solution and requires protection from atmospheric dioxygen. Controlled oxidation of $[(ODTDPP)Fe^{II}(C_6H_5)_2]^-$ with Br_2 yields $[(ODTDPP)Fe^{III}(C_6H_5)Br]$ **5**, which presents the typical ^1H NMR features of a low-spin σ-aryl iron(III) porphyrin (Figure 5).[29,34]

Paradoxically, the oxidation reaction mechanism may involve the reduction step to generate the known iron(I) oxaporphyrin intermediate as shown in Scheme 2. Hypothetically, one-electron oxidation yields $(ODTDPP)Fe^{III}(C_6H_5)_2$, which is expected to be readily reduced in a two-

Scheme 2. Oxidation of 3-H

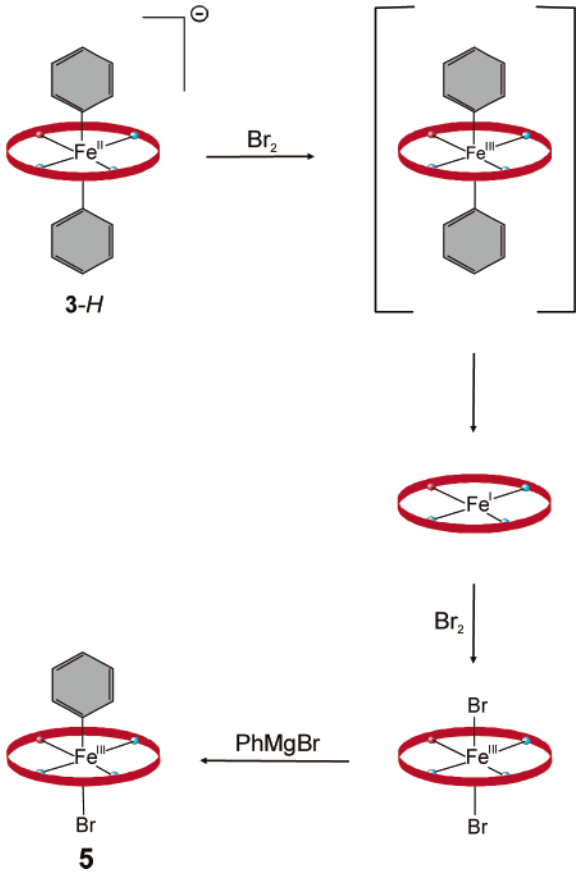

electron process. Eventually in the presence of Br_2 and the Grignard reagent this reaction stops at the formation of **5**.

While the spectroscopic properties of **3**-H are consistent with the [(ODTDPP)Fe^{II}(C_6H_5)$_2$]$^-$ stoichiometry, the electronic structure of the compound remains to be discussed. The pattern of ^{1}H NMR spectra of **3** is unlike those of any other paramagnetic σ-aryliron porphyrin and σ-aryliron heteroporphyrins now known.[19,26,29,30,34,46,48] Note that [(ODTDPP)Fe^{II}(C_6H_5)$_2$]$^-$ can be prepared starting with the high-spin iron(II) 21-oxaporphyrin (ODTDPP)Fe^{II}Br. Alternatively, the stepwise addition of the aryl Grignard to (ODTDPP)Fe^{III}Br$_2$ originally results in the formation of (ODTDPP)Fe^{II}Br species, which is then converted into [(ODTDPP)Fe^{II}(C_6H_5)$_2$]$^-$ **3**-H. Significantly, the treatment of (ODTDPP)Fe^{III}Br$_2$ with two equivalents of PhMgBr yields (ODTDPP)Fe^{I} directly and cleanly at 205 K characterized by distinct ^{1}H NMR spectrum as described in detail previously.[19] We have also found that the iron(I) 21-oxaporphyrin (ODTDPP)Fe^{I} could not be detected once (ODTDPP)Fe^{II}Br has been used as a substrate in titration with aryl Grignard reagents. Significantly the heterolytic dissociation of [(ODTDPP)Fe^{II}(C_6H_5)$_2$]$^-$ yields (ODTDPP)Fe^{II}(C_6H_5), and the redox reactions are clearly not a part of the chemistry that occurs here. It is unlikely that Fe(III) is involved since we definitely observe reduction occurring during the addition of the Grignard reagent to (ODTDPP)Fe^{III}Br$_2$. The pattern of ^{1}H shifts does not correspond to any previously observed σ-aryliron(III) porphyrins. Another possibility could include Fe(I), which is d^7, but the known spectroscopic features of (ODTDPP)Fe^{I} and the fact that the iron(I) species does not coordinate any axial ligand exclude such a possibility.[19] Concluding, only the iron(II) oxidation state is consistent with the detected reactivity of [(ODTDPP)Fe^{II}(C_6H_5)$_2$]$^-$ **3**-H.

^{1}H NMR studies of high-spin iron(II) porphyrins demonstrated that the dipolar contribution to the paramagnetic shift is rather small.[38,49−54] The contact shift pattern is consistent with the high-spin electronic structure $(d_{xy})^2(d_{xz})^1(d_{yz})^1(d_{z^2})^1(d_{x^2-y^2})^1$ and a dominance of a σ-delocalization mechanism. An additional contribution of π-delocalization mechanism in the porphyrin ring was also noted.[53,54] Usually the indication of the significant role of the contact shift for tetraarylporphyrins can be derived from the shift pattern of *meso*-aryl resonances. It was shown that in the paramagnetic complexes of porphyrins and their analogues this pattern depends on whether the contact or dipolar shift dominates.[34] In particular, the contact shift mediated by π orbitals of the *meso*-aryl results in a characteristic sign alteration of the shifts experienced by the ortho, meta, and para protons of the *meso*-phenyls. In the present case the shift pattern displayed by the identified meso substituent signals (5.55 ppm (ortho) 5.90 ppm (para), other resonances are hidden under the intense solvent signals) confirm that the dipolar contribution is negligible. To show qualitatively that the observed spread of shifts is not a result of dipolar contribution, we have assumed a purely dipolar shift of σ-aryl resonances and performed geometric factor calculations adjusting the orientation of the main magnetic axis along Fe−C_{ipso}. The predicted order of the paramagnetic shifts: ortho > meta > *p*-CH_3 is clearly inconsistent with the experimental spectra.

Generally, the straightforward and unambiguous correlation between the ^{1}H NMR pattern and the molecular and electronic structure has been determined for paramagnetic metalloporphyrins and metalloheteroporphyrins containing the σ-aryl ligand.[19,26,29,34,46,48] Usually, the protons of a phenyl σ-bounded to a five-coordinated Ni(II) display substantial downfield contact shifts (Table 1), which are indicative of the σ-contact contribution and is consistent with the $(d_{xy})^2(d_{xz})^2(d_{yz})^2(d_{z^2})^1(d_{x^2-y^2})^1$ ground electronic state and the presence of the unpaired electron on the d_{z^2} orbital.[9,14,15,55] The isotropic shifts of the equatorial ligand are also dominated by the same effect revealing resonances in the 0−60 ppm region. The examination of the isotropic shifts for low-spin σ-phenyliron(III), $(d_{xy})^2(d_{xz},d_{yz})^3(d_{z^2})^0(d_{x^2-y^2})^0$ [26,29,34,46,48]; σ-phenyliron(IV), tetraarylporphyrins $((d_{xy})^2(d_{xz})^1(d_{yz})^1(d_{z^2})^0(d_{x^2-y^2})^0$ [30]; and σ-phenylruthenium(IV) octaethylporphyrin, $(d_{xy})^2(d_{xz})^1(d_{yz})^1(d_{z^2})^0(d_{x^2-y^2})^0$ [47] indicated a large amount of π-spin density at the axial phenyl ligand

(48) Kadish, K. M.; Tabard, A.; Lee, W.; Liu, Y. H.; Ratti, C.; Guilard, R. *Inorg. Chem.* **1991**, *30*, 1542.
(49) Goff, H. M.; La Mar, G. N. *J. Am. Chem. Soc.* **1977**, *99*, 6599.
(50) Mispelter, J.; Momenteau, M.; Lhoste, J. M. *Biochimie* **1981**, *63*, 911.
(51) Latos-Grażyński, L. *Biochimie* **1983**, *65*, 143.
(52) Medhi, O. K.; Mazumdar, S.; Mitra, S. *Inorg. Chem.* **1989**, *28*, 3243.
(53) Yu, B.-S.; Goff, H. M. *J. Am. Chem. Soc.* **1989**, *111*, 6558.
(54) Shin, K.; Kramer, K.; Goff, H. M. *Inorg. Chem.* **1987**, *26*, 4103.
(55) Chmielewski, P. J.; Latos-Grażyński, L. *Inorg. Chem.* **2000**, *39*, 5639.

because of overlapping of d_{xz} and/or d_{yz} orbitals with occupied π orbitals of axial aryl(s). Thus, the σ-aryl contains unpaired electron(s), but the d_{z^2} orbital is not occupied. Some contribution of the σ-mechanism was also suggested.[9] The marked upfield shifts for ortho and para resonances and the downfield shift for the meta is typical of such a mechanism.[34]

Qualitatively the ^{1}H NMR pattern detected for **3** can be viewed as a hybrid of two extremes described above, suggesting the possibility of coexistence of σ and π delocalization mechanisms. For that reason, the relatively small downfield isotropic shifts of the σ-*p*-tolyl protons (60−20 ppm), which decrease in the peculiar order of meta > *p*-CH_3 > ortho, have been determined for **3**-Me. Contrary to *p*-CH_3 of the **3**-Me signal, the para-H resonance of **3**-H is located in an upfield position. Thus the replacement of the proton by the methyl group produces the contact shift of the opposite sign, as expected for the π-delocalization mechanism. The peculiar spectral features of **3** indicate a profound alteration of the electronic structure of iron(II) ion upon the coordination of two σ-phenyls (Figures 2 and 4, Table 1). The upfield positions of the β-H macrocycle resonances imply the domination of the π spin delocalization mechanism that involves the π-orbital framework of 21-oxaporphyrin.[34] The pattern is indicative of a negligible σ-contact contribution and is consistent with the absence of unpaired electron on the $d_{x^2-y^2}$ orbital. Hence, the iron(II) d orbitals that contribute to the single occupied molecular orbitals must be those of π-symmetry (i.e., d_{xz} and d_{yz}). An interpretation of this spin delocalization requires a change of the metal ion ground state from $(d_{xy})^2(d_{xz})^1(d_{yz})^1(d_{z^2})^1(d_{x^2-y^2})^1$ that is common for high-spin iron(II) macrocycles including the monoaryl adduct **2** to involve sizable contributions of $(d_{xy})^2(d_{x^2-y^2})^2(d_{yz})^1(d_{xz})^1(d_{z^2})^0$, $(d_{xy})^2(d_{x^2-y^2})^2(d_{yz},d_{xz})^1(d_{z^2})^1$ ($S = 1$), $(d_{x^2-y^2})^2(d_{z^2})^1(d_{xy})^1(d_{yz})^1(d_{xz})^1$ ($S = 2$), or $(d_{x^2-y^2})^2(d_{z^2})^1(d_{xy})^1(d_{yz})^1(d_{xz})^1$ ($S = 2$) electronic configurations for **3**, respectively. Alternatively, one can consider three electronic structures involving the d_{z^2} orbital, and left unoccupied $d_{x^2-y^2}$ one: $(d_{xy})^2(d_{yz})^1(d_{xz})^1(d_{z^2})^2(d_{x^2-y^2})^0$, $(d_{xy})^2(d_{yz})^1(d_{xz})^2(d_{z^2})^1(d_{x^2-y^2})^0$, $(d_{xy})^2(d_{yz})^2(d_{xz})^1(d_{z^2})^1(d_{x^2-y^2})^0$ ($S = 1$). Such a profound transformation of the ground electronic state cannot be accounted for merely by a choice of σ- or π-donating properties of the aryl ligand but results primarily from the simultaneous coordination of two σ-aryl ligands. One can note that the coordination of a single aryl yields predictably high-spin (ODTDPP)$Fe^{II}(C_6F_5)$ **2** and diamagnetic (ODTDPP)$Fe^{II}(C_6H_5)$ **4**.[56] Consistently (ODTDPP)$Fe^{III}(C_6H_5)$Br **5** presents the typical spectrum of low-spin σ-aryliron(III) porphyrins.[26,29,34,46,48] Stabilization of the less-common paramagnetic ground electronic state of the six-coordinate iron(II) can be rationalized on the basis of effective and simultaneous σ- and π-aryl donation to the iron. As a result the d_{xz}, d_{yz}, and d_{z^2} orbitals acquire similar energy, affording one of the electronic configurations described above. For the sake of comparison, it is worth to admit that four-coordinate iron(II) porphyrins favor the electronic configuration $(d_{xy})^2(d_{z^2})^2(d_{yz},d_{xz})^2$.[57] The existence of an intermediate spin state for six-coordinate iron(II) complexes was also reported and explained in terms of a major distortion from the octahedral symmetry and degeneracy of one-electron d_{xz}, d_{yz}, and d_{z^2} orbitals.[58] Although the available NMR data do not permit further characterization of the electronic state of the thermally unstable σ-aryl(II) 21-oxaporphyrin **3**, they clearly identify the peculiar ground electronic state of iron(II) porphyrins, which definitely requires extensive theoretical studies.

Now we can return to the discussion of the two other bis-(σ-phenyl) paramagnetic metalloporphyrin systems where the electronic state, as characterized by ^{1}H NMR spectroscopy, revealed the unusual features in comparison to the "regular" σ-monoaryl species. Thus $(O_2TPP)Ni^{II}(C_6H_5)_2$ presents the strongly upfield position of β-H pyrrole (−143.1 ppm) and furan (−31.35 ppm) resonances accompanied by rather minor isotropic shifts of σ-aryls (ortho 5.5, meta, −4.47 ppm, 243 K).[14] The pattern of σ-phenyl resonances assigned for the six-coordinate verdoheme complex $[(OEOP)Fe(Ph)_2]^-$ (ortho, −6.5, meta, 43; para, 10 ppm, 203 K) resembles the one determined in this work for $[(ODTDPP)Fe^{II}(C_6H_5)_2]^-$.[33] Consequently, the comparison of the spectroscopic properties of $[(ODTDPP)Fe^{II}(C_6H_5)_2]^-$ and $[(OEOP)Fe(C_6H_5)_2]^-$ seems to favor the less-common ground electronic state of iron(II) in the verdoheme case as well.

In conclusion, the modification of the porphyrin core by the introduction of an oxygen atom seems to be crucial for stabilization of the organometallic derivatives of iron(II). The nature of the equatorial ligand seems to be instrumental in determining the stoichiometry of organoiron(II) species trapped at low temperature. The ^{1}H NMR spectral pattern of **3** reveals the less-common ground electronic state of iron-(II) porphyrins. Previously the variations of the spin density sings of β-H resonances were reported for five-coordinate high-spin core modified iron(II) porphyrins including *N*-alkyl porphyrins.[38,49] This work documents the peculiar case where the axial coordination to iron(II) switches the sign of spin density for each β-position. Thus the unique ^{1}H NMR spectrum of **3** provides a new entry to the increasing collection of paramagnetic iron(II) porphyrins.

The recent reports on high-spin iron(II) hemoproteins are of particular interest in light of our findings. These studies provided a detailed assignment of resonances of the heme pocket for *Rhodobacter capsulatus* ferrocytochrome *c*′,[59] ferrous *Aplysia limacine*,[60] and ferrous mamalian myoglobins.[61] Consequently, these allowed a firm separations of the contact and dipolar shifts. Significantly, the sign alternations of spin densities at the adjacent pyrolic β-positions have been unambiguously established for ferrocytochrome *c*′ [59] and *A. limacine* myoglobin.[60] In contrast, the uniformly positive spin density at all β-pyrrole positions was determined for ferrous mamalian myoglobins.[61] As discussed above, the available

(56) Tahiri, M.; Doppelt, P.; Fischer, J.; Weiss, R. *Inorg. Chem.* **1988**, *27*, 2897.
(57) Goff, H. M.; La Mar, G. N. *J. Am. Chem. Soc.* **1977**, *99*, 6606.
(58) Figg, D. C.; Herber, R. H.; Felner, I. *Inorg. Chem.* **1991**, *30*, 2535.
(59) Tsan, P.; Caffrey, M.; Lawson Daku, L.; Cusanovich, M.; Marion, D.; Gans, P. *J. Am. Chem. Soc.* **1999**, *121*, 1795.
(60) Ma, D.; Musto, R.; Smith, K. M.; La Mar, G. N. *J. Am. Chem. Soc.* **2003**, *125*, 8494.
(61) Bougault, C. M.; Dou, Y.; Ikeda-Saito, M.; Langry, K. C.; Smith, K. M.; La Mar, G. N. *J. Am. Chem. Soc.* **1998**, *120*, 2113.

and typical spectroscopic models—high-spin five coordinate iron(II) porphyrins—demonstrate the low-field positions of β-H and methyl resonances as clearly found in deoxy myoglobins.[61] The compounds considered in this paper made it clear that the upfield β-H contact shift is evidently acceptable for axially coordinate iron(II) porphyrins.

Experimental Section

Preparation of Compounds. The iron(II) 21-oxaporphyrins (ODTDPP)Fe^{II}Cl **1** and (ODTDPP-d_6)Fe^{II}Cl **1**-d_6 were prepared as described previously.[19] Grignard reagents (C_6H_5)MgBr, (C_6D_5)MgBr (C_6F_5)MgBr, (*p*-$CH_3C_6H_4$)MgBr, and (4-F−C_6H_4)MgBr as solutions in diethyl ether (Aldrich) have been used as received.

Phenylmagnesium Bromide Addition to 1. Samples for spectroscopic study were prepared in dioxygen-free solvents under dinitrogen atmosphere in a glovebox. Sample concentration for the iron complexes were in the range 1−3 mM. The sample was placed in a 5 mm NMR tube and carefully sealed with a septum cap. In the case of low-temperature studies, the sample was removed from the glovebox and cooled to 195 K in the ethanol bath, which was chilled by the addition of sufficient amount of liquid nitrogen to reach 195 K. Subsequently aliquots of a 1 M solution of phenylmagnesium bromide (or other Grignard reagent in diethyl ether) were introduced into the sample through the microsyringe. The sample was shaken in the cold bath and transferred to the precooled NMR probe, and the progress of the reaction was followed by ^{1}H NMR spectroscopy.

Instrumentation. All NMR spectra were recorded on a Bruker Avance 500 spectrometer operating in the quadrature mode. An exponential window function has been applied to improve the signal-to-noise ratio. The residual ^{1}H resonances of the deuterated solvents were used as secondary references.

Acknowledgment. This work was supported by the State Committee for Scientific Research of Poland (KBN) under Grant 4 T09A 147 22.

IC0495463